Structure of incommensurate NiTi(Fe)

Ian Folkins and M. B. Walker
Department of Physics, University of Toronto, Toronto, Ontario, Canada M5S 1A7
(Received 19 December 1988; revised manuscript received 16 March 1989)

NiTi(Fe) has an incommensurate and a commensurate phase between its low-temperature martensitic and high-temperature CsCl-type structures. Anomalous deviations of the satellite positions in the incommensurate phase have been reported. These deviations have raised doubts about the adequacy of a model based on sinusoidal modulations of the basic structure. Our Landau model shows that these features can be explained by considering the coupling of the modulations to the lattice strain.

I. INTRODUCTION

Nickel titanium has a martensitic phase transition at 273 K. The space-group symmetry of the martensitic phase has been established as $P2_1/m$.[1-4] However, the symmetries occurring in a series of structural changes extending 20 K above T_M remain controversial, despite having been the subject of experimental study for over twenty years.[5-10] Further, it is not known what, if any, is the physical connection between these changes and the martensitic phase transition. Obviously, a knowledge of the structure of NiTi in the pretransitional region is a prerequisite to the establishment of such a relation.

Since 1976, most experiments have been done on NiTi(Fe).[11-15] The dilute Fe, which replaces a small percentage of the Ni, strongly depresses T_M while leaving the onset temperature of the pretransitional region approximately unchanged. The expansion of the pretransitional region allows its features to be distinguished from those associated with the growth of the martensite. Our model is devoted to explaining observations reported in $Ni_{46.8}Ti_{50}Fe_{3.2}$ by Shapiro *et al.*[12] At present, it is not clear that our conclusions apply to NiTi itself.[5-6]

The high-temperature phase of NiTi(Fe) has, on average,[16] the space group $Pm\bar{3}m$. The Bravais lattice is simple cubic, with one of the two types of atoms considered to be occupying the corners of the cubes with the other at their centers. At an initial transition temperature $T_{\rm I}$, satellites belonging to the stars of $q_{\rm I}$ and $q_{\rm II}$ appear. The wave vectors $q_{\rm I}$ and $q_{\rm II}$ are approximately given by $\frac{1}{3}(1,1,0)$ and $\frac{1}{3}(1,1,1)$, respectively. Early experiments found small deviations from $\frac{1}{3}$, so that $q_{\rm I}$ and $q_{\rm II}$ were incommensurate. A later experiment by Shapiro *et al.*[12] found that it was impossible to index the satellites by any set of wave vectors. The deviation of a satellite from its commensurate position depends on the zone in which it is found. Higher-order satellites tend to be located further from their associated Bragg peak than their lower-order counterparts. The deviation pattern, $\delta(\mathbf{Q})$, is given in Figs. 2(a) and 3(a).

A second pretransitional phase transition appears at $T_{\rm II}$. Here the satellites lock to commensurate positions and there is a discontinuous rhombohedral distortion. As the temperature is reduced below $T_{\rm II}$, the amount of rhombohedral distortion continuously increases. Transmission electron microscopy (TEM) pictures[13] indicate the existence of four domains. Within each domain only those $q_{\rm I}$ satellites appear whose $\mathbf{q}$ vectors are perpendicular to one of the four rhombohedral directions. Further, the only $q_{\rm II}$ satellite seen is the one parallel to this direction. At T_M, the crystal starts to convert to a martensite.

We shall refer to the phase between $T_{\rm I}$ and $T_{\rm II}$ as the incommensurate phase. The identification of its structure is the main task of this paper. The phase between $T_{\rm II}$ and T_M is referred to as the commensurate phase. $T_{\rm I}$, $T_{\rm II}$, and T_M are 232 K, 224 K, and 110 K, respectively, for $Ni_{46.8}Ti_{50}Fe_{3.2}$.[12]

A variety of evidence indicates that the transition to the incommensurate phase is second order. Both the $q_{\rm I}$ and $q_{\rm II}$ satellites appear to grow continuously at $T_{\rm I}$ and there is no temperature hysteresis in their disappearance.[12-14] Further, there is no anomaly in the specific heat at $T_{\rm I}$.[14] We assume in our Landau model that the transition is in fact second order and set the coefficient of the quadratic term equal to zero at $T_{\rm I}$.

The major challenge in devising a structural model for incommensurate NiTi(Fe) is to account for the idiosyncratic deviations $\delta(\mathbf{Q})$ in the satellite positions. To some, this has implied the destruction of three-dimensional order. Yamada *et al.*[17-18] have suggested that the existence and positions of the satellites can be explained by nucleations of martensite within the high temperature phase. Salamon *et al.*[14] devised a lattice discommensuration model motivated by the observation that the satellite deviations in the [001] zone were directed toward rhombohedral positions. There has also been a suggestion of analogies to ω-phase behavior.[12] But none of these three proposals have generated a three-dimensional model that has been compared with the full range of experimental data.

Our model assumes that the satellites correspond to sinusoidal modulations of the basic structure of the high-temperature phase. It takes the amplitudes of these modulations to be the primary order parameters. It then demonstrates how the occurrence of these primary order parameters must necessarily induce some rhombohedral lattice distortion. This arises from the destruction of cu-

bic symmetry caused by the modulations. The resulting rhombohedral strains are secondary order parameters.

If the rhombohedral distortion gives rise to domains, its effect on the positions of the Bragg peaks and those of the satellites will be different. A rhombohedral distortion will not cause a net movement of the Bragg peaks. This is because the new peaks from each domain distribute themselves symmetrically about the old cubic positions. For a small distortion, the splitting of these peaks would be difficult to observe. The satellites, however, will be seen to move under a rhombohedral distortion. This is because a given satellite is always associated with one or two of the four possible domains. It must then be referenced with respect to the rhombohedral Bragg peaks of its particular domain(s), rather than the average Bragg positions which are still cubic. Taking this into consideration enables us to account for the observed $\delta(\mathbf{Q})$.

The existence of a rhombohedral distortion in the incommensurate phase has been controversial. Salamon *et al.*[14] found no deviation of the rhombohedral angle α from 90.0° between $T_{\rm I}$ and $T_{\rm II}$. In $Ni_{47}Ti_{50}Fe_3$ however, movements of the Bragg peaks below $T_{\rm I}$ were found to be suggestive of a rhombohedral distortion in the incommensurate phase.[19] Later studies found the same result for $Ni_{46.8}Ti_{50}Fe_{3.2}$ as well.[20]

Our model can be considered an extension of that proposed by Shapiro *et al.*[12] They also understood the primary symmetry lowering to have been brought about by sinusoidal $q_{\rm I}$ modulations. This largely explained both the $q_{\rm I}$ and $q_{\rm II}$ satellite intensities. However they could not explain the $\delta(\mathbf{Q})$ that they measured nor extinctions [see Fig. 3(a)] of the $q_{\rm II}$ satellites in the $[01\bar{1}]$ zone. Nevertheless, the amount of agreement obtained was thought to indicate an approximation of the actual structure. Our model accounts for the deviations in the satellite positions. The problem of the apparently random $q_{\rm II}$ extinctions is not addressed here, though it is conceivable that they may be accounted for by our model.

In Sec. II, the Landau free energy consistent with the symmetry of the high-temperature phase is derived. The transformation properties of the order parameters are derived from those of their associated modes. Thus much of Sec. II is devoted to defining the relevant modes. The formalism given here is related to that previously used by one of us to describe the modulated phases of α-uranium.[21] In Sec. III it is shown how the fourth-order free energy allows a second-order transition to an incommensurate three-q rhombohedral state. The physically inequivalent choices of phase for the nonzero order parameters are then classified. In Sec. V it is shown how a three-q rhombohedral state gives rise to accompanying rhombohedral strains. The effect of these strains on the satellite positions is explained in Sec. VI. Sec. VII consists of preliminary observations on the relevance of the Landau expansion to the commensurate phase. Section VIII is a summary of our conclusions.

II. DERIVATION OF THE FREE ENERGY

To allow for the incommensurability of the $\mathbf{q}_{\rm I}$ satellites, let $\xi=\frac{1}{3}-\delta$. Then the following six vectors, plus their negatives, form the star of wave vector $\xi(1,\bar{1},0)$:

$$\begin{aligned} &\mathbf{q}_1=\xi(1,1,0), \quad \mathbf{q}_4=\xi(1,\bar{1},0)\ , \\ &\mathbf{q}_2=\xi(0,1,1), \quad \mathbf{q}_5=\xi(0,1,\bar{1})\ , \\ &\mathbf{q}_3=\xi(1,0,1), \quad \mathbf{q}_6=\xi(\bar{1},0,1)\ . \end{aligned} \tag{1}$$

The notation $\mathbf{q}_j^0$ will refer to the same $\mathbf{q}$ vectors with $\delta=0$. The modes with these $\mathbf{q}$ vectors will be written as linear combinations of the basis vectors $e(l,s,\alpha)$. The basis vector $e(l,s,\alpha)$ represents the state of the crystal with a displacement of unity of atom s in unit cell l in direction α. Here s can be 0 or $\frac{1}{2}$, with 0 referring to the atom at the center of the simple-cubic unit cell, and with $\frac{1}{2}$ to the atom at its corner. The equilibrium position of an atom can then be represented as $\mathbf{R}(l,s)=(l_1+s)\mathbf{a}_1+(l_2+s)\mathbf{a}_2+(l_3+s)\mathbf{a}_3$. The simple-cubic Bravais-lattice vectors $\mathbf{a}_1$, $\mathbf{a}_2$, and $\mathbf{a}_3$ are in the [100], [010], and [001] directions, respectively. One now defines vectors which are a basis for a one-dimensional irreducible representation of the crystal's translation group:

$$e(\mathbf{q},s,\alpha)=N^{-1/2}\sum_l e^{i\mathbf{q}\cdot\mathbf{R}(l,s)}e(l,s,\alpha)\ . \tag{2}$$

When acted upon by an element of the crystal's translation group, they transform according to

$$\{E|\mathbf{R}(l)\}e(\mathbf{q},s,\alpha)=e^{-i\mathbf{q}\cdot\mathbf{R}(l)}e(\mathbf{q},s,\alpha)\ . \tag{3}$$

A general distortion with periodicity $\mathbf{q}_1^0$ will be an arbitrary linear combination of the six $e(\mathbf{q}_1^0,s,\alpha)$. The mode $e(\mathbf{q}_1^0)$ which gives rise to the $\mathbf{q}_1^0$ satellites is known[14] to have TA_2 symmetry. It transforms according to the Σ_4 irreducible representation[22] of the little cogroup of $\mathbf{q}_1^0$. Imposition of this symmetry, and also of time-reversal symmetry, determines $e(\mathbf{q}_1^0)$. The remaining five $e(\mathbf{q}_j^0)$ can then be found by application of the appropriate point-group element to $e(\mathbf{q}_1^0)$. All six $e(\mathbf{q}_j^0)$ are given in Appendix A.

The transformation properties of the $e(\mathbf{q}_j^0)$ under a set of generators of $Pm\bar{3}m$ can be shown to be

$$\{I|\mathbf{0}\}e(\mathbf{q}_j^0)=e^*(\mathbf{q}_j^0)\ , \tag{4a}$$

$$\{C_{31}|\mathbf{0}\}e(\mathbf{q}_j^0)=e(C_{31}\mathbf{q}_j^0)\ , \tag{4b}$$

$$\{C_{4z}|\mathbf{0}\}e(\mathbf{q}_j^0)=\exp[i\mathbf{q}_j^0\cdot\tfrac{1}{2}\mathbf{c}]e(C_{4z}\mathbf{q}_j^0)\ , \tag{4c}$$

$$\{E|\mathbf{a}_i\}e(\mathbf{q}_j^0)=\exp[-i\mathbf{q}_j^0\cdot\mathbf{a}_i]e(\mathbf{q}_j^0)\ . \tag{4d}$$

The convention for the phases of the $e(\mathbf{q}_j^0)$ has been chosen so that the normal modes satisfy Eq. (4a). The six $e(\mathbf{q}_j^0)$, plus their complex conjugates, are a basis for an irreducible corepresentation of $Pm\bar{3}m$. The matrices of this corepresentation are defined by Eqs. (4).

The most general way of characterizing distortions of the type given by the $e(\mathbf{q}_j^0)$ is through the state vector $\mathbf{u}$,

$$\mathbf{u}=\mathrm{Re}\left\{\sum_{j=1}^{6}[\psi_j(\mathbf{r})e(\mathbf{q}_j^0)]\right\}\ . \tag{5}$$

The order parameters $\psi_j(\mathbf{r})$ are complex functions of position. A good approximation close to $T_{\rm I}$ is to consider

only the first harmonic:

$$\psi_j(\mathbf{r})=|\psi_j|e^{i(\mathbf{p}_j\cdot\mathbf{r}+\phi_j)} . \quad (6)$$

The introduction of the $\mathbf{p}_j$ allows us to consider state vectors representing incommensurate distortions, despite having defined the modes as commensurate. This is because the wave vector $\mathbf{p}_j$ of the order parameter and $\mathbf{q}_j^0$ of the $e(\mathbf{q}_j^0)$ simply add to give a total wave vector of $\mathbf{q}_j^0+\mathbf{p}_j$. To see this, let $\psi_1(\mathbf{r})$ be of the form given by Eq. (6), with all other $\psi_j(\mathbf{r})=0$. Now derive the atomic displacement pattern $u(l,s,\alpha)$ from $\mathbf{u}$. Expand $e(\mathbf{q}_1^0)$ first in terms of the $e(\mathbf{q}_1^0,s,\alpha)$, and then in terms of the $e(l,s,\alpha)$. Then substitute $\mathbf{R}(l,s)$ for $\mathbf{r}$. The $u(l,s,\alpha)$ are the coefficients of the $e(l,s,\alpha)$.

$$u(l,s,\alpha)=-a_s|\psi_1|(\mathbf{e})_\alpha\sin[(\mathbf{q}_1^0+\mathbf{p}_1)\cdot\mathbf{R}(l,s)+\phi_1] \quad (7)$$

The state vector $\mathbf{u}$ transforms under a space-group operation according to

$$\{P|\mathbf{w}\}\mathbf{u}=\mathrm{Re}\left[\sum_{j=1}^{6}\psi_j(\{P|\mathbf{w}\}^{-1}\mathbf{r})\{P|\mathbf{w}\}e(\mathbf{q}_j^0)\right] . \quad (8)$$

An identical effect on the atomic displacements can be obtained by operating solely on the order parameters. For instance, it is not difficult to verify that if $\psi_j(\mathbf{r})\rightarrow\psi_j^*(\mathbf{r})$ under inversion, the effect on $\mathbf{u}$ is the same as that achieved by using Eq. (4a) in Eq. (8). The transformation properties of the order parameters under the generators of $Pm\bar{3}m$ can be derived in this way. They are given in Appendix B. The free-energy density, up to invariant terms of fourth order or less, can then be shown to be[23]

$$F=\sum_{j=1}^{6}\psi_j^*(\mathbf{r})A_j(-i\nabla)\psi_j(\mathbf{r})+B_1\left[\sum_{j=1}^{6}|\psi_j|^2\right]^2+B_2\left[\sum_{j=1}^{6}|\psi_j|^4\right]$$
$$+B_3(|\psi_1|^2|\psi_4|^2+|\psi_2|^2|\psi_5|^2+|\psi_3|^2|\psi_6|^2)+B_4[(\psi_1\psi_4\psi_6\psi_3^*+\psi_1\psi_4^*\psi_5^*\psi_2^*+\psi_6\psi_3\psi_5\psi_2^*)+(\mathrm{c.c.})] . \quad (9)$$

An expansion to this order can be expected to be accurate close to T_I. B_1, B_2, B_3, and B_4 are assumed to be constants independent of temperature.[24]

We assume that the order parameters have the form given by Eq. (6) close to T_I. Their spatial variation is then completely prescribed by their $\mathbf{p}_j$. Hence,

$$A_j(-i\nabla)\psi_j(\mathbf{r})=A_j(\mathbf{p}_j)\psi_j(\mathbf{r}) . \quad (10)$$

The point group symmetry of the Brillouin zone ensures that $A_j(\mathbf{p}_j)$ will be extremal along the $\mathbf{q}_j^0$ directions in reciprocal space. It is therefore likely that the minima of $A_j(\mathbf{p}_j)$ will occur along these directions as well. As indicated in the introduction, this agrees with experiment. However, there is no symmetry to make $A_j(\mathbf{p}_j)$ extremal at the $\mathbf{q}_j^0(\mathbf{p}_j=\mathbf{0})$. Its minima will therefore occur at incommensurate reciprocal distances from the $\mathbf{q}_j^0$. These reciprocal distances will be referred to as $-3\,\delta\mathbf{q}_j^0$. Assuming the transition at T_I to be second order, the $A_j(-3\,\delta\mathbf{q}_j^0)$ will pass through zero at T_I. Hence to first order near T_I, the $A_j(-3\,\delta\mathbf{q}_j^0)$ will vary with temperature as

$$A_j(-3\,\delta\mathbf{q}_j^0)=k(T-T_\mathrm{I}) \quad (11)$$

where k is a positive constant. Thus, just below T_I, the order parameters will have the form given by Eq. (6) and will prescribe distortions with incommensurate wave vectors $\mathbf{q}_j$.

III. THE PHASE DIAGRAM

We specialize to those states whose nonzero $|\psi_j|$ are equal. Further, we consider only those for which the $\mathbf{q}_j$ of their nonzero $|\psi_j|$ sum to zero. The minimum free energy of a given state with n nonzero equal $|\psi_j|$ can be calculated. It will be some function of the four B's. The global minimum can be found by comparing these functions for different n. The resulting phase diagram is shown in Fig. 1. Only the $B_4=0$ plane is shown. A nonzero B_4 tends to favor a four- or six-$\mathbf{q}$ state and for large enough B_4, only these states will be stable. The diagram also assumes $B_1>0$. For $B_1<0$, only a six-$\mathbf{q}$ state is possible.

Note that a three-$\mathbf{q}$ state will be favored for $B_1,B_2>0$, B_3 large enough, and B_4 small. The four degenerate three-$\mathbf{q}$ rhombohedral domains will be referred to as the {456}, {423}, {513}, and {612} states. Each of the four domains has only those $\psi_j(\mathbf{r})$ nonzero whose q vectors are perpendicular to their rhombohedral direction. Since experiments have indicated that the incommensurate

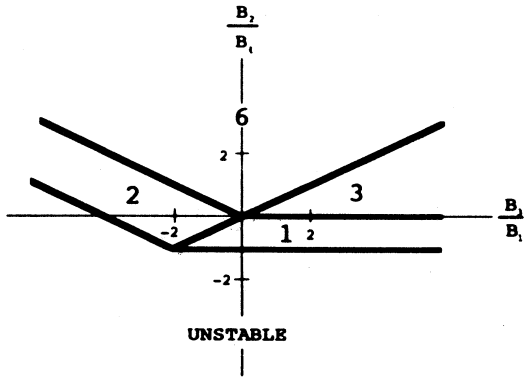

FIG. 1. The regions of stability of the 1, 2, 3 and six-$\mathbf{q}$ states in the $B_4=0$ plane. B_1 is taken to be positive. Note that there is a region of parameter space in which the three-$\mathbf{q}$ rhombohedral state is stable.

phase does have this form, we will restrict our attention to these states from now on. In particular, we shall refer mainly to the {456} domain.

There are in fact four other, less symmetrical three-**q** states that are degenerate with the three-**q** rhombohedral states in the fourth-order free energy of Eq. (9). The sixth-order terms (see Appendix C) however break this degeneracy. And it can be shown that for the D_1 coefficient of the D_1 term sufficiently big, the three-**q** rhombohedral states are always favored.

IV. THE INCOMMENSURATE PHASES

Although the free-energy density given by Eq. (9) allows for a transition to a rhombohedral incommensurate state, it does not completely prescribe the symmetry of these states. This is because it does not distinguish between rhombohedral states of differing phases. To determine the possible phases, it is necessary to consider the sixth-order invariants. There are twelve such terms. They can be found in Appendix C. It can be shown that the only term which constrains the rhombohedral incommensurate phases is the D_1 term. For incommensurate {456} order parameters of the form given by Eq. (6), it reduces to

$$2D_1|\psi_4\psi_5\psi_6|^2\cos[2(\phi_4+\phi_5+\phi_6)] . \tag{12}$$

It is always possible to smoothly translate the modulation pattern of a crystal in those directions in which it is incommensurate without changing its symmetry or free energy. Such a translation is equivalent to varying the appropriate phase. The phases of the order parameters of incommensurate crystals are therefore never entirely specified. This freedom is made manifest by writing the phases as $\phi_j=\phi_{j0}-\mathbf{q}_j\cdot\mathbf{r}_0$. From the definition of the state vector, it can be shown that a change of $\delta\mathbf{r}_0$ in $\mathbf{r}_0$ corresponds to sliding the modulation pattern with respect to the basic structure by the same amount. The rhombohedral {456} state is incommensurate in the plane defined by its three incommensurate **q** vectors. The vector $\mathbf{r}_0$ may therefore take on any value within this plane. It remains then to specify the ϕ_{j0}. These are chosen so as to minimize the D_1 term. For each of the two choices of sign for D_1, it can be shown that there are only two physically inequivalent choices for the ϕ_{j0}. The total of four possible cases have $\phi_{j0}=\phi_0$, where ϕ_0 is 0 or $\pi/3$ for $D_1<0$, and ϕ_0 is $\pi/6$ or $\pi/2$ for $D_1>0$.

Although we have considered only the {456} states in this section, a similar analysis of the incommensurate phases would apply to the three other domains.

V. THE RHOMBOHEDRAL STRAIN

A rhombohedral distortion is described by off-diagonal (shear) strains. Their transformation properties under the $Pm\bar{3}m$ generators are given in Appendix B. These properties can be used to find the lowest-order strain-to-order parameter and strain-to-strain invariant terms. They are

$$N[e_6(|\psi_1|^2-|\psi_4|^2)+e_5(|\psi_3|^2-|\psi_6|^2)+e_4(|\psi_2|^2-|\psi_5|^2)]+\frac{C_{44}}{2}(e_6^2+e_5^2+e_4^2) . \tag{13}$$

The strains and elastic constant have been labeled with Voigt notation.[25] $C_{44}>0$ is required for stability. The order parameters, being primary, prescribe the symmetry of the incommensurate state. Therefore, to find the strains appropriate to a {456} state, take $|\psi_4|=|\psi_5|=|\psi_6|=|\psi|$, with all other $|\psi_j|=0$. The coupling is indifferent to the phases to this order. Then the off-diagonal strains which minimize (13) are

$$e_4=e_5=e_6=\frac{N}{C_{44}}|\psi|^2 . \tag{14}$$

These strains describe a rhombohedral distortion in the [111] direction. This relation between the q_I satellite intensities and the magnitude of the rhombohedral strain can be expected to be accurate close to T_I. This is the regime where the two terms in Eq. (13) make the dominant contribution of the strains to the free energy. Because their net contribution is negative, nonzero off-diagonal strains will always occur in the three-**q** rhombohedral states. They will give rise to an elongation or compression along the rhombohedral axis depending on whether N is positive or negative.

Experiments indicate that the elastic constant C_{44} increases with temperature.[26,27] According to Eq. (14), this would then contribute to the increase in the rhombohedral distortion below T_I.

The diagonal strains can also be shown to couple to the primary order parameters. This coupling is not considered here because, to lowest order, it simply induces an isotropic volume change which has no effect on the symmetry.

VI. THE EFFECT OF A RHOMBOHEDRAL STRAIN ON THE SATELLITE POSITIONS

If the four rhombohedral domains were present in approximately equal amounts, there would be no net movement of the Bragg peaks. One would expect to see only a progressive broadening and eventually splitting of peaks as one moved to higher and higher zones. The satellites however will be displaced by a rhombohedral distortion. The distortion matrices for each of the rhombohedral domains are given in Appendix D. They will be used to calculate the satellite deviations $\delta(\mathbf{Q})$. We will confine our attention to the [001] and [01$\bar{1}$] zones as these have been investigated by experiment.[12]

The distortion matrices B give the new $\mathbf{x}'$ to which a position vector **x** moves after a distortion by a rhombohedral angle of α.

$$\mathbf{x}'=\mathsf{B}\mathbf{x} \tag{15}$$

The angle α will always be within a degree of 90° in incommensurate NiTi(Fe). A good approximation is to write the matrix entries to first order in $\epsilon=\frac{1}{2}(\pi/2-\alpha)$. Doing this, and rewriting them to define movements in

reciprocal rather than real space, gives the reciprocal distortion matrices B_R. They are given in Appendix D.

Let **Q** label the cubic Bragg peak to which a satellite **q** is referenced. The deviation of the satellite from its commensurate cubic position is then

$$\delta(\mathbf{Q}\pm\mathbf{q}^0)=B_R(\mathbf{Q}\pm\mathbf{q})-(\mathbf{Q}\pm\mathbf{q}^0)\ . \tag{16}$$

A complication arises when a satellite is associated with more than one domain. All q_{I} satellites, for example, derive scattering intensity from two of the four domains. The ambiguity in the choice of B_R means the deviation is not unique. This is a source of anisotropy in the satellite widths. (The incommensurateness of the **q** vectors may also give rise to anisotropy, as will be shown later for the q_{II} satellites).

One would expect to see in the [001] zone those satellites whose **q** vectors are perpendicular to the [001] direction. This is satisfied for $\mathbf{q}_4$. These satellites come from the {456} and {423} domains. The deviation will be different for each. However, as their differences are confined to the [001] direction they will not give rise to anisotropy in the [001] zone. The deviation is found by using Eq. (16) and the reciprocal distortion matrices given in Appendix D. Taking $L=0$ for the [001] zone,

$$\begin{aligned}
\{423\}:\ \delta\left[\begin{pmatrix}H\\K\\0\end{pmatrix}\pm\mathbf{q}_4^0\right]&=-\epsilon\begin{pmatrix}K\\H\\-H-K\end{pmatrix}\pm\left[\frac{\epsilon}{3}-\delta\right]\begin{pmatrix}1\\-1\\0\end{pmatrix},\\
\{456\}:\ \delta\left[\begin{pmatrix}H\\K\\0\end{pmatrix}\pm\mathbf{q}_4^0\right]&=-\epsilon\begin{pmatrix}K\\H\\H+K\end{pmatrix}\pm\left[\frac{\epsilon}{3}-\delta\right]\begin{pmatrix}1\\-1\\0\end{pmatrix}.
\end{aligned} \tag{17}$$

A term going as $\epsilon\delta$ has been dropped. Both domains have identical deviation in the [100] and [010] directions. Hence there is no anisotropy of the satellite widths in the [001] zone.

The major qualitative features of the deviation are accounted for by the first of the two terms on the right of Eq. (17). They are compared with the actual [001] zone deviation in Fig. 2. The agreement in the directionality is excellent. The second terms in Eqs. (17) introduce a small uniform shift rather than a deviation that varies from zone to zone. They will be taken into consideration when calculating the best ϵ and δ that numerically fit the data.

In the $[01\bar{1}]$ zone, q_{II} satellites occur at reciprocal distances of approximately $\pm\frac{1}{3}(1,1,1)$ and $\pm\frac{1}{3}(-1,1,1)$ from the (HKK) Bragg peaks. The deviations of both can be explained in the same way as for the q_{I} satellites. In addition the widths of these satellites are anisotropic. This can be ascribed to the incommensurateness of the q_{I} satellites.

The q_{II} satellites can be understood as second-order q_{I} satellites. Their scattering intensity will then have two physically different sources. One source will be first-order harmonics of the q_{I} wave vectors. These were assumed small in Sec. II, but as secondary order parame-

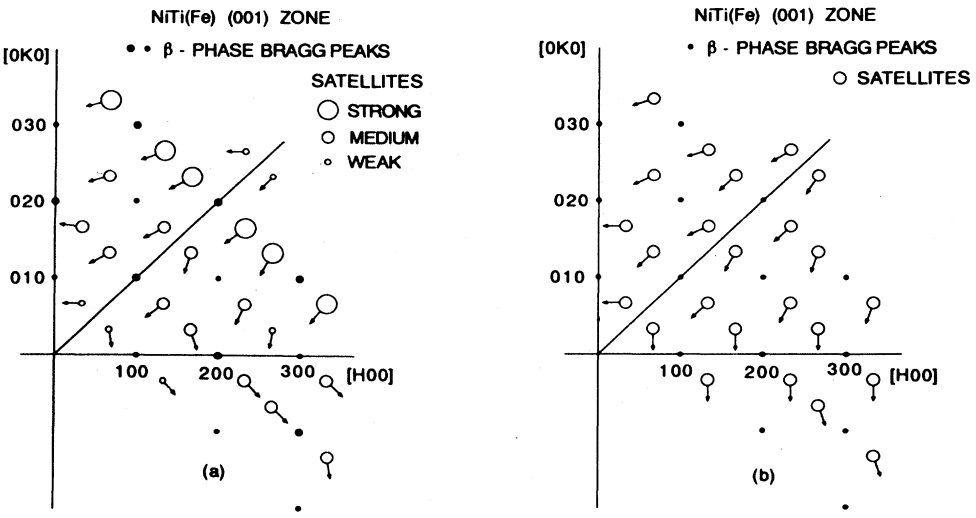

FIG. 2. (a) The [001]-zone $\mathbf{q}_4$ satellite intensities and deviations taken from Ref. 12. Only the direction of the deviation is given. The length of the arrows is not significant. (b) Our approximate deviation directions.

ters, they will always occur to some extent. However, as demonstrated in Ref. 12, the q_{II} satellites will appear independently of whether harmonics are present or not. This is because the density function is a nonlinear function of the atomic displacements.

The position of a q_{II} satellite is independent of its source. The q_{II} vector of a particular domain is always constructed from two of its q_I vectors and a reciprocal-lattice vector. There are, however, always three inequivalent ways of doing this. For example, the three ways of constructing the $\frac{1}{3}(1,1,1)$ satellite of the $\{456\}$ domain are

$$\tfrac{1}{3}(1,1,1)=\begin{cases}\mathbf{q}_5^0-\mathbf{q}_6^0+(0,0,1)\,, & \text{(18a)}\\ \mathbf{q}_4^0-\mathbf{q}_5^0+(0,1,0)\,, & \text{(18b)}\\ \mathbf{q}_6^0-\mathbf{q}_4^0+(1,0,0)\,. & \text{(18c)}\end{cases}$$

The deviation of a $\pm\frac{1}{3}(1,1,1)$ satellite from its (HKK) Bragg peak depends on which of the three constructions is used. Using the same technique as for the q_I satellites, the deviation for the three cases can be shown to be

$$\delta\left[\begin{bmatrix}H\\K\\K\end{bmatrix}\pm\tfrac{1}{3}(1,1,1)\right]=-\epsilon\begin{bmatrix}2K\\H+K\\H+K\end{bmatrix}\mp\frac{2\epsilon}{3}\begin{bmatrix}1\\1\\1\end{bmatrix}$$

$$\pm\begin{cases}\delta\begin{bmatrix}-1\\-1\\2\end{bmatrix}\,, & \text{(19a)}\\ \delta\begin{bmatrix}-1\\2\\-1\end{bmatrix}\,, & \text{(19b)}\\ \delta\begin{bmatrix}2\\-1\\-1\end{bmatrix}\,. & \text{(19c)}\end{cases}$$

Again, terms of order $\epsilon\delta$ have been dropped.

The first term on the right of Eq. (19) gives the dominant contribution to the deviation. The pattern it gives rise to is compared with that found experimentally in Fig. 3. Again the agreement is very good. The first two terms taken together define the average deviation of the $\pm\frac{1}{3}(1,1,1)$ satellite. The third term indicates that it actually consists of three distinct satellites distributed symmetrically about this average position. They lie in the plane perpendicular to the [111] direction. This should be made manifest in the $[01\bar{1}]$ zone as an elongation of the satellite widths in the $[\bar{2}11]$ direction. From Fig. 4 of Shapiro *et al.*[12] it can be seen that this is the case.

The analysis of the $\pm\frac{1}{3}(-1,1,1)$ satellite deviations is identical to that of the $\pm\frac{1}{3}(1,1,1)$ deviations. The average deviation of a $\pm\frac{1}{3}(-1,1,1)$ satellite is

$$\delta\left[\begin{bmatrix}H\\K\\K\end{bmatrix}\pm\frac{1}{3}\begin{bmatrix}-1\\1\\1\end{bmatrix}\right]=\epsilon\begin{bmatrix}2K\\H-K\\H-K\end{bmatrix}\pm\frac{2\epsilon}{3}\begin{bmatrix}1\\-1\\-1\end{bmatrix}\,. \quad (20)$$

This can be compared with the deviation of the two $\pm\frac{1}{3}(-1,1,1)$ satellites shown in Fig. 4 of Shapiro *et al.*[12] The agreement is again excellent.

There are actually three $\pm\frac{1}{3}(-1,1,1)$ satellites symmetrically distributed about the average deviation given by Eq. (20). They lie in the plane perpendicular to the $[\bar{1}11]$ direction. This should reveal itself in the $[01\bar{1}]$ zone as an elongation of the satellite widths in the [211] direction. Figure 4 of Shapiro *et al.*[12] shows that there is indeed some elongation of the two $\frac{1}{3}(-1,1,1)$ satellites shown, though the alignment with the [211] direction is imperfect.

Equations (17) and (19) predict the deviation for the $\mathbf{q}_4$ and $\pm\frac{1}{3}(1,1,1)$ satellites in terms of the two parameters ϵ and δ. It is possible to determine the ϵ and δ that best fit the actual deviations found in Figs. 3 and 4 of Shapiro *et al.*[12] The determination is crude because the deviations are comparable to the widths of the satellites themselves. But with $\epsilon=0.0023$ and $\delta=0.0011$, Eq. (17) correctly specified $\delta(\mathbf{Q}\pm\mathbf{q}_4)$ to within 50% of 16 of 22 deviation directions. The correspondence for the eight $\pm\frac{1}{3}(1,1,1)$ satellites in the $[01\bar{1}]$ zone was somewhat better. With the same ϵ, Eq. (19) achieved the same accuracy for 14 of 16 deviation directions. From the definition of ϵ, $\epsilon=0.0023$ is equivalent to a rhombohedral angle of $\alpha=89.7°$.

VII. THE COMMENSURATE PHASE

As the order parameters increase in magnitude below T_I, the free-energy expansion to fourth order in order parameters given by Eq. (9) will progressively lose validity. In this case, the sixth-order terms may alter the symmetry of the equilibrium phase. These terms are given in Appendix D. Of particular interest are the terms with coefficients D_2, D_3, and D_4. With incommensurate order parameters of the form given by Eq. (6), they are periodic functions of position. Their contribution to the free energy therefore averages to zero when integrated over the entire crystal. If the crystal is commensurate however, $\mathbf{p}_j=\mathbf{0}$ and the three terms become constants. They may induce the crystal to become commensurate if their contribution to the free energy is sufficiently negative. We suggest that the lock-in transition at T_{II} is indeed driven by the D_2, D_3, and D_4 sixth order umklapp terms.

The space group of the commensurate phase is determined by the phases ϕ_j of the order parameters. These, in turn, are determined by the D_1, D_2, D_3, and D_4 terms. A detailed analysis of the resulting phase diagram is complex. However, it can be shown that the two choices $\phi_j=0$ and $\phi_j=\pi/2$ each minimize the four terms for particular values of the D's. These correspond to the space groups $P\bar{3}$ and $P3lm$, respectively. Both space groups have been previously discussed by Shapiro *et al.*[12] in relation to the incommensurate phase.[28] Subgroups of these space groups are also conceivable.

A convergent beam electron diffraction experiment has assigned the symmetry $P\bar{3}lm$ to the commensurate phase of $Ni_{47}Ti_{50}Fe_3$.[10] But because there are no phases for which the order parameters have this symmetry, this symmetry is not consistent with the results of our theory.

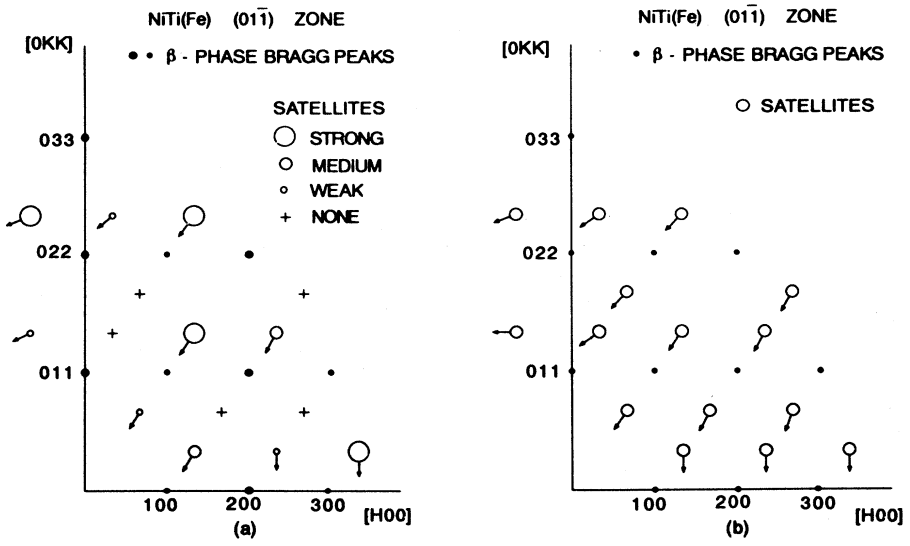

FIG. 3. (a) The [01$\bar{1}$]-zone $\frac{1}{3}(1,1,1)$ satellite intensities and deviations taken from Ref. 12. Only the direction of the deviation is given. The length of the arrows is not significant. (b) Our approximate satellite deviation directions.

VIII. CONCLUSIONS

Anomalous deviations of the incommensurate satellite positions from commensurate positions are observed in NiTi(Fe). A number of attempts to explain these deviations have been made, all of which, up to the present, have invoked explanations which lie outside the framework of a conventional theoretical treatment of incommensurate crystals. This article has shown that, provided one acknowledges the existence of different incommensurate domains in a given crystal, and provided that one takes account of the different strains (relative to the cubic phase) which exist in these different domains, one can account in some detail for the anomalous satellite deviations within the framework of a conventional theory of the incommensurate phase.

There are a variety of other ways in which our theory could be further tested. The most direct way would be to perform a diffraction experiment on a single domain sample. One way in which such a sample may be created is by cooling it through the normal to incommensurate phase transition temperature in a stress sufficiently large and in such a direction as to preferentially favor the formation of one of the four domains. Failing this there are a number of indirect methods. One could, for example, test our theoretical relations between the rhombohedral angle and the satellite deviations and intensities, or between the anisotropic $q_{\rm II}$ satellite widths and the incommensurateness of the $q_{\rm I}$ wave vectors. This latter relation has already been shown to be approximately correct. Further measurements should verify its quantitative accuracy.

ACKNOWLEDGMENTS

This research was supported by the Natural Sciences and Engineering Research Council of Canada.

APPENDIX A

Gooding *et al.*[29] have formulated a Landau theory of the $\frac{1}{3}(1,-1,0)$ mode in Li. Because Li has the same point group as NiTi(Fe), our Landau expansions should be almost identical. We have adopted their conventions regarding the normal modes and the order parameter transformation properties. However, our Landau expansion has more terms, theirs being incomplete. One of the new terms found here is crucial to our work since it is responsible for stabilizing the three-**q** state.

Let $\mathbf{e}=(-1,1,0)$ and $P_j\mathbf{e}$ be the new polarization vector into which **e** is transformed by the point-group operation P_j. The αth component of this vector is then $(P_j\mathbf{e})_\alpha$. The six $e(\mathbf{q}_j^0)$ are then

$$e(\mathbf{q}_j^0)=i\sum_\alpha [a_0(P_j\mathbf{e})_\alpha e(\mathbf{q}_j^0,0,\alpha) + a_{1/2}(P_j\mathbf{e})_\alpha e(\mathbf{q}_j^0,\tfrac{1}{2},\alpha)] .$$

The P_j are defined as $P_1=E$, $P_2=C_{31}^{-1}$, $P_3=C_{31}$, $P_4=C_{4z}$, $P_5=C_{4y}^{-1}$, $P_6=C_{4x}^{-1}C_{4z}$, and a_0 and $a_{1/2}$ are real constants.

APPENDIX B

The transformation properties of the order parameters can be found by using the procedure outlined in Sec. II. Under a set of $Pm\bar{3}m$ generators, they are

$$\{E|\mathbf{a}_i\}\psi_j(\mathbf{r})=\exp[-i\mathbf{q}_j^0\cdot\mathbf{a}_i]\psi_j(\mathbf{r}) ;$$

$$\{I|\mathbf{0}\}\psi_j(\mathbf{r})=\psi_j^*(\mathbf{r}) ;$$

$$\{C_{31}|\mathbf{0}\}:\ \psi_1\to\psi_2\to\psi_3\to\psi_1 ,\quad \psi_4\to\psi_5\to\psi_6\to\psi_4 ;$$

$$\{C_{4z}|\mathbf{0}\}:\ \psi_1\to\psi_4^*\to\psi_1^*\to\psi_4\to\psi_1 ,\quad \psi_2\to\psi_6\to-\psi_5^*\to-\psi_3\to\psi_2 .$$

The transformation properties under $\{C_{31}|\mathbf{0}\}$ and $\{C_{4z}|\mathbf{0}\}$ have been represented as orbits. Those of the shear strains $e_i, i=4, 5, 6$, can be similarly represented.

$$\{I|\mathbf{0}\}e_i=\{E|\mathbf{0}\}e_i=e_i \ ;$$

$$\{C_{31}|\mathbf{0}\}: \ e_4\rightarrow e_5\rightarrow e_6\rightarrow e_4 \ ;$$

$$\{C_{4z}|\mathbf{0}\}: \ e_6\rightarrow -e_6\rightarrow e_6 \ ,$$

$$e_5\rightarrow e_4\rightarrow -e_5\rightarrow -e_4\rightarrow e_5 \ .$$

APPENDIX C

The twelve sixth-order invariant terms can be found by using the transformation properties of the order parameters given in Appendix B. They are

$$\begin{aligned}
F^6=&D_1\{[A^2+B^2+C^2+D^2]+[\text{c.c.}]\}\\
&+D_2\{[(\psi_1^3-\psi_4^3)(\psi_3^3-\psi_6^{*3})+(\psi_1^3-\psi_4^{*3})(\psi_2^3-\psi_5^3)+(\psi_2^3-\psi_5^{*3})(\psi_3^3-\psi_6^3)]+(\text{c.c.})\}\\
&+D_3\{[(\psi_1^3-\psi_4^3)(\psi_3^{*3}-\psi_6^3)+(\psi_1^{*3}-\psi_4^3)(\psi_2^3-\psi_5^3)+(\psi_2^{*3}-\psi_5^3)(\psi_3^3-\psi_6^3)]+(\text{c.c.})\}\\
&+D_4\sum_{j=1}^{6}(\psi_j^6+\psi_j^{*6})+D_5\sum_{j=1}^{6}|\psi_j|^6\\
&+D_6[(\psi_1^3+\psi_1^{*3})(\psi_4^3+\psi_4^{*3})+(\psi_2^3+\psi_2^{*3})(\psi_5^3+\psi_5^{*3})+(\psi_3^3+\psi_3^{*3})(\psi_6^3+\psi_6^{*3})]\\
&+D_7\{(|\psi_1|^2+|\psi_4|^2)(|\psi_2|^2+|\psi_3|^2+|\psi_5|^2+|\psi_6|^2)\\
&\qquad+(|\psi_2|^2+|\psi_5|^2)(|\psi_1|^2+|\psi_3|^2+|\psi_4|^2+|\psi_6|^2)+(|\psi_3|^2+|\psi_6|^2)(|\psi_1|^2+|\psi_2|^2+|\psi_4|^2+|\psi_5|^2)\}\\
&+D_8(AA^*+BB^*+CC^*+DD^*)\\
&+D_9(|\psi_1|^2|\psi_2|^2|\psi_3|^2+|\psi_2|^2|\psi_4|^2|\psi_6|^2+|\psi_3|^2|\psi_4|^2|\psi_5|^2+|\psi_1|^2|\psi_5|^2|\psi_6|^2)\\
&+D_{10}[(|\psi_1|^2+|\psi_4|^2)(|\psi_3|^2|\psi_6|^2+|\psi_2|^2|\psi_5|^2)\\
&\qquad+(|\psi_2|^2+|\psi_5|^2)(|\psi_3|^2|\psi_6|^2+|\psi_1|^2|\psi_4|^2)\\
&\qquad+(|\psi_3|^2+|\psi_6|^2)(|\psi_2|^2|\psi_5|^2+|\psi_1|^2|\psi_4|^2)]\\
&+D_{11}[(AB+AC+AD+BC^*+BD^*+CD^*)+(\text{c.c.})]\\
&+D_{12}[(A^*B+A^*C+A^*D+BC+BD+CD)+(\text{c.c.})] \ .
\end{aligned}$$

A, B, C, and D represent

$$A=\psi_4\psi_5\psi_6, \quad C=\psi_5\psi_1^*\psi_3 \ ,$$

$$B=\psi_4\psi_2\psi_3^*, \quad D=\psi_6\psi_1\psi_2^* \ .$$

The notation c.c. represents the complex conjugate of the term in its neighboring bracket.

APPENDIX D

The deviation of any satellite can be found by using Eq. (16). The appropriate distortion and reciprocal distortion matrices for each domain are given below.

Domain	Rhombohedral axis	B	B_R
{456}	[111]	$\begin{bmatrix} m & -n & -n \\ -n & m & -n \\ -n & -n & m \end{bmatrix}$	$\begin{bmatrix} 1 & -\epsilon & -\epsilon \\ -\epsilon & 1 & -\epsilon \\ -\epsilon & -\epsilon & 1 \end{bmatrix}$
{135}	$[\bar{1}11]$	$\begin{bmatrix} m & n & n \\ n & m & -n \\ n & -n & m \end{bmatrix}$	$\begin{bmatrix} 1 & \epsilon & \epsilon \\ \epsilon & 1 & -\epsilon \\ \epsilon & -\epsilon & 1 \end{bmatrix}$
{162}	$[1\bar{1}1]$	$\begin{bmatrix} m & n & -n \\ n & m & n \\ -n & n & m \end{bmatrix}$	$\begin{bmatrix} 1 & \epsilon & -\epsilon \\ \epsilon & 1 & \epsilon \\ -\epsilon & \epsilon & 1 \end{bmatrix}$
{423}	$[\bar{1}\bar{1}1]$	$\begin{bmatrix} m & -n & n \\ -n & m & n \\ n & n & m \end{bmatrix}$	$\begin{bmatrix} 1 & -\epsilon & \epsilon \\ -\epsilon & 1 & \epsilon \\ \epsilon & \epsilon & 1 \end{bmatrix}$

A derivation of the distortion matrices is given in Miyazaki *et al.*[30] From there,

$m = (2\sqrt{2}/3)\sin(\alpha/2) + [3 - 4\sin^2(\alpha/2)]^{1/2}/3$,

$n = (\sqrt{2}/3)\sin(\alpha/2) - [3 - 4\sin^2(\alpha/2)]^{1/2}/3$.

The rhombohedral angle α is geometrically defined in Ref. 30. The parameter ϵ is defined in Sec. VI.

[1]G. M. Michal and R. Sinclair, Acta Crystallogr. Sect. B **37**, 1803 (1981).

[2]W. Bührer, R. Gotthardt, A. Kulik, O. Mercier, and F. Staub, J. Phys. F **13**, L77 (1983).

[3]K. Kudoh, M. Tokonami, S. Miyazaki, and K. Otsuka, Acta Metall. **33**, 2049 (1985).

[4]O. Matsumoto, S. Miyazaki, K. Otsuka, and H. Tamura, Acta Metall. **35**, 2137 (1987).

[5]H. Tietze, M. Müllner, P. Selgert, and W. Assmus, J. Phys. F **15**, 263 (1985).

[6]H. Tietze, M. Müllner, and B. Renker, J. Phys. C **17**, L529 (1984).

[7]G. D. Sandrock, A. J. Perkins, and R. F. Hehemann, Metall. Trans. **2**, 2769 (1971).

[8]P. M. Moine, G. M. Sinclair, and R. Sinclair, Acta Metall. **30**, 109 (1982).

[9]G. M. Michal, P. Moine, and R. Sinclair, Acta Metall. **30**, 125 (1982).

[10]E. Goo and R. Sinclair, Acta. Metall. **33**, 1717 (1985).

[11]M. Matsumoto and T. Honma, *New Aspects of Martensitic Transformations, First JIM International Symposium on Martensite, Kobe, 1976* (Japan Institute of Metals, Kobe, 1976).

[12]S. M. Shapiro, Y. Noda, Y. Fujii, and Y. Yamada, Phys. Rev. B **30**, 4314 (1984).

[13]C. M. Hwang, M. Meichle, M. B. Salamon, and C. M. Wayman, Philos. Mag. A **47**, 9, 31, 177 (1983).

[14]M. B. Salamon, M. E. Meichle, and C. M. Wayman, Phys. Rev. B **31**, 7306 (1985).

[15]S. K. Satija, S. M. Shapiro, M. B. Salamon, and C. M. Wayman, Phys. Rev. B **29**, 6031 (1984).

[16]The presence of the iron will cause localized deviations from pure $Pm\bar{3}m$ symmetry. We assume that the main effect of these deviations on our Landau expansion is to perturb the parameters from their pure NiTi values.

[17]Y. Yamada, Metall. Trans. A **19A**, 777 (1988).

[18]Y. Yamada, Y. Noda, and M. Takimoto, Solid State Commun. **55**, 1003 (1985).

[19]S. M. Shapiro, Metall. Trans. A **12**, 567 (1981).

[20]S. M. Shapiro (unpublished).

[21]M. B. Walker, Phys. Rev. B **34**, 6830 (1986).

[22]C. J. Bradley and A. P. Cracknell, *The Mathematical Theory of Symmetry in Solids* (Clarendon, Oxford, 1972).

[23]The parameters in the Landau expansion are here considered to have all renormalizations due to secondary order parameters implicitly included. The order parameters are then considered to represent the state of the crystal which minimizes the free energy for those particular modulations. In Sec. V we consider explicitly the contribution of the shear strains to the free energy. This is done to find the strains appropriate to the three-**q** rhombohedral states. Because the strains are secondary order parameters, they will have no effect on the phase diagram derived in this section.

[24]This assumption is not strictly true. The temperature dependence of the C_{44} elastic constant (Refs. 26 and 27) will mean that at least some of the fourth order parameters are temperature dependent as well. Though this could make the transition at T_1 first order, experimental evidence appears to indicate that it does not.

[25]R. A. Cowley, Phys. Rev. B **13**, 4877 (1976).

[26]O. Mercier, K. N. Melton, G. Gremaud, and J. Hägi, J. Appl. Phys. **51**, 1833 (1980).

[27]V. N. Khachin, S. A. Muslov, V. G. Pushin, and Yu. I. Chumlyakov, Dokl. Akad. Nauk SSSR **292**, 606 (1987) [Sov. Phys. Dokl. **32**, 606 (1987)].

[28]Their space group assignments to the two sets of phases appear opposite to ours due to differences in convention.

[29]R. J. Gooding and J. A. Krumhansl, Phys. Rev. B **38**, 1695 (1988).

[30]S. Miyazaki, S. Kimura, and K. Otsuka, Philos. Mag. A **57**, 467 (1988).